Ferromagnetic In-Plane Spin Fluctuations in Na_xCoO_2 Observed by Neutron Inelastic Scattering

A. T. Boothroyd,[1,*] R. Coldea,[1] D. A. Tennant,[2] D. Prabhakaran,[1] L. M. Helme,[1] and C. D. Frost[3]
[1]*Department of Physics, Oxford University, Oxford, OX1 3PU, United Kingdom*
[2]*School of Physics and Astronomy, University of St. Andrews, St. Andrews, Fife, KY16 9SS, United Kingdom*
[3]*ISIS Facility, Rutherford Appleton Laboratory, Chilton, Didcot, OX11 0QX, United Kingdom*
(Received 23 December 2003; published 13 May 2004)

We present neutron scattering spectra taken from a single crystal of $Na_{0.75}CoO_2$, the precursor to a novel cobalt-oxide superconductor. The data contain a prominent inelastic signal at low energies ($\sim$10 meV), which is localized in wave vector about the origin of two-dimensional reciprocal space. The signal is highly dispersive, and decreases in intensity with increasing temperature. We interpret these observations as direct evidence for the existence of ferromagnetic spin fluctuations within the cobalt-oxygen layers.

DOI: 10.1103/PhysRevLett.92.197201 PACS numbers: 75.40.Gb, 74.20.Mn, 74.25.Ha, 78.70.Nx

Sodium cobalt oxide (Na_xCoO_2) has become of considerable interest in the past few years owing first to the report of a large thermoelectric power coupled with low resistivity in single crystals of $Na_{0.5}CoO_2$ [1] and, second, to the serendipitous discovery of superconductivity at temperatures below $T_c \simeq 5$ K in $Na_xCoO_{2\cdot y}H_2O$ ($x \simeq 0.3$, $y \simeq 1.3$) formed by hydration of precursor Na_xCoO_2 [2]. The enhanced thermoelectric properties of Na_xCoO_2 make it potentially important for technological applications, and the existence of superconductivity in the hydrated compound raises very interesting questions about the pairing mechanism in relation to the cuprate and ruthenate superconductors.

Like the superconducting cuprates and ruthenates, the structure of Na_xCoO_2 is layered, consisting in this case of triangular CoO_2 sheets separated by layers of Na^+ ions. Incorporation of water increases the sheet separation and decreases the Na content. Metallic behavior is achieved by doping the Mott-insulating CoO_2 sheets with electrons donated by Na, which create Co^{3+} ions with zero spin in a background of Co^{4+} carrying spin $S = \frac{1}{2}$. The enhanced thermopower has been ascribed to a large spin entropy arising from strong electron-electron interactions in the CoO_2 sheets [3].

Superconductivity in the hydrated compound is observed in a narrow range of composition centered around $x = 0.3$ [4]. Although the pairing mechanism has not yet been established, a number of experimental studies have uncovered evidence suggesting that the superconductivity in this material is unconventional [5]. Several attempts [6–10] to understand the superconductivity have been based on Anderson's resonating valence bond (RVB) idea [11], which describes a singlet quantum spin liquid ground state stabilized by frustration. The $S = \frac{1}{2}$ triangular lattice could in principle support an RVB state providing the coupling between nearest-neighbor spins were antiferromagnetic, as suggested by the high temperature susceptibility of both superconducting $Na_{0.35}CoO_2 \cdot 1.3H_2O$ [12] and precursor Na_xCoO_2 [13]. Among alternative scenarios, the possibility of spin-triplet superconductivity has been analyzed by several authors [6,14–16], and has received support from resonance experiments [5]. The existence of ferromagnetic correlations, which would open the door to p-wave spin-triplet pairing, was predicted from density-functional calculations for Na_xCoO_2 with $x = 0.3$–0.7 [17,18]. The predicted ferromagnetic instability was found to be robust to the structural changes associated with hydration [18]. Proximity to a ferromagnetic instability is suggested by an irreversible magnetic transition at $T_m = 22$ K in Na_xCoO_2 [19], an upturn in the low temperature susceptibility of Na_xCoO_2 [19,20] and $Na_{0.35}CoO_2 \cdot 1.3H_2O$ [12], and has also been inferred from some nuclear relaxation measurements [5].

The importance of spin degrees of freedom, both to explain the thermopower and in most of the theories of superconductivity proposed thus far, makes it essential to have experimental information on magnetic correlations, especially to establish whether the dominant in-plane coupling is ferromagnetic or antiferromagnetic. This information can most directly be obtained from neutron scattering measurements on single crystal samples. Crystals of superconducting compositions large enough for neutron scattering are not yet available. Here we present the first neutron inelastic scattering spectra of the precursor compound Na_xCoO_2. The data provide strong evidence for the existence of ferromagnetic spin correlations within the CoO_2 layers.

Single crystals of $Na_{0.75}CoO_2$ were grown by the floating-zone method in an image furnace [20]. A crystal of size $\sim 10 \times 8 \times 3$ mm^3 was cleaved from the zone-melted rod. Magnetization and powder x-ray diffraction measurements made on samples taken from adjacent parts of the same crystal rod showed no impurity phases within the detectable limit of $\sim$2%.

Neutron inelastic scattering measurements were made on the MAPS spectrometer at the ISIS Facility. MAPS is a

time-of-flight instrument equipped with a large pixellated detector surrounding the incident beam direction. Neutrons of well-defined incident energy are delivered to the sample in short pulses. Spectra in each pixel are recorded as a function of neutron time of flight, and, subsequently, transformed into an intensity array in ($\mathbf{Q}$, E) space, where $\mathbf{Q} = \mathbf{k}_i - \mathbf{k}_f$ is the scattering vector (the difference between the incident and final neutron wave vectors) and E is the energy transferred to the sample. The intensity was converted into an absolute cross section by comparison with the scattering from vanadium. The presented spectra are the partial differential cross section $d^2\sigma/d\Omega dE_f$ per formula unit (f.u.) multiplied by the factor k_i/k_f [21], where E_f is the final energy.

The crystal was attached to a copper rod and mounted on a closed-cycle cooler. Measurements were made at several temperatures between 6 K and room temperature. Typical counting times were 36 h at an average proton current of 170 μA. An initial examination by neutron Laue diffraction showed that the crystal contained several grains with an overall mosaic spread of $\sim 10°$. To maintain good $\mathbf{Q}$ resolution, we employed relatively low incident energies ($E_i = 40$ meV and 60 meV), and restricted our measurements to small scattering angles.

The physical properties of Na_xCoO_2 are highly two dimensional (2D) [1]. It is likely, therefore, that any magnetic correlations between the CoO_2 layers are very weak, and, hence, that the magnetic scattering is relatively insensitive to the component of $\mathbf{Q}$ parallel to the crystal c axis. For an initial survey, therefore, we aligned the crystal with the c axis parallel to the incident neutron beam, so that the area detector recorded the energy spectrum over a large region of 2D reciprocal space (>1 Brillouin zone) spanned by the $\mathbf{a}^*$ and $\mathbf{b}^*$ reciprocal lattice basis vectors of the triangular lattice in the CoO_2 plane [22]. The energy range probed in this configuration was from 2 to 50 meV. By taking a series of constant-energy slices, we made a search of ($\mathbf{Q}_{2D}$,E) space, where $\mathbf{Q}_{2D} = h\mathbf{a}^* + k\mathbf{b}^* \equiv (h, k)$ is the in-plane component of the scattering vector. The only signal we found that was clearly in excess of the background in this energy range was distributed symmetrically around the unscattered beam, i.e., $\mathbf{Q}_{2D} = (0, 0)$. In particular, there was no observable signal at wave vectors corresponding to antiferromagnetic correlations between adjacent Co sites.

To investigate the observed signal further, we rotated the crystal by 30°, so that more of the $\mathbf{Q}_{2D} = (0, 0)$ scattering would be recorded in the detectors adjacent to the unscattered beam. Figure 1 displays the neutron intensity averaged over the energy range 8–12 meV and projected onto the a^*b^* plane. The unscattered beam passes through the center of the blank rectangle where there are no detectors. The map shows an enhanced signal roughly twice the background in the detectors to the right of the blank rectangle. This is the same signal observed in the unrotated orientation, but now it has shifted to the right due to the rotation of the crystal. This confirms that the signal is centered on $\mathbf{Q}_{2D} = (0, 0)$; part of the signal is missing where it overlaps the blank rectangle. Away from this feature the intensity landscape is featureless. We remark here that the peak is much broader in wave vector than the resolution. The latter is dominated by the crystal mosaic, which causes a spread in wave vector of $\sim 0.05a^*$ at this energy, whereas the peak has a width of $\sim 0.2a^*$.

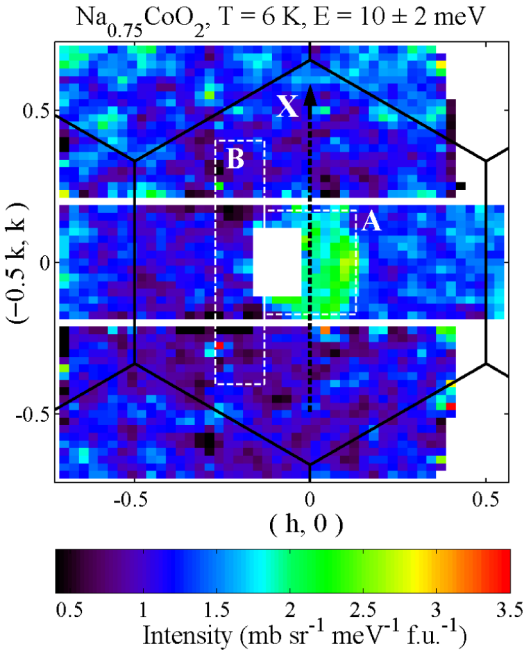

FIG. 1 (color online). Neutron inelastic scattering from $Na_{0.75}CoO_2$ recorded in the MAPS spectrometer area detector with $E_i = 60$ meV. The image is a plot of $(k_i/k_f)d^2\sigma/d\Omega dE_f$ per formula unit (f.u.), averaged between energies of 8 and 12 meV, and projected onto the (h, k) plane in reciprocal space. Blocks of missing data are due to gaps between detector banks. The hexagonal grid plotted over the data shows the 2D Brillouin zone boundaries. The two rectangular boxes marked A and B are the areas over which data were averaged for the scans in Fig. 2. The vertical dotted line marked X indicates the line along which the cuts shown in Figs. 3 and 4 were taken.

Figure 2 shows the energy dependence of the scattering measured at a temperature of 6 K. To construct this scan, we averaged the data over a rectangular box (marked A in Fig. 1) centered on (0, 0) enclosing the peak. Two distinct features stand out above the background: (1) a peak centered near 20 meV, and (2) an increase in scattering with decreasing energy below 15 meV. The signal appears to level off below 10 meV, but this trend cannot be established definitively from the current data because at low energies a significant proportion of the signal is lost where there are no detectors, as can be seen in Fig. 1.

Measurements made at higher temperatures revealed that the two features just described behave very differently with temperature. The key findings are illustrated in

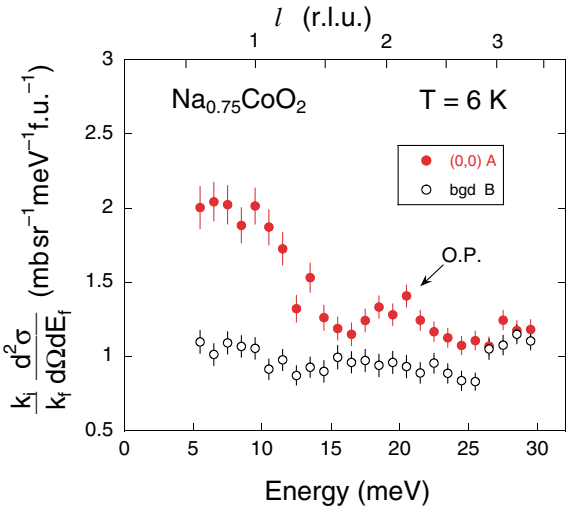

FIG. 2 (color online). Energy dependence of the scattering from $Na_{0.75}CoO_2$. Filled circles are data averaged over the rectangular box marked A in Fig. 1 centered on $\mathbf{Q}_{2D} = (0, 0)$. The background signal has been estimated from the region marked B in Fig. 1. The out-of-plane wave vector component $l\mathbf{c}^*$ is marked on the upper axis in reciprocal lattice units (r.l.u.) for the scan centered on (0, 0). The peak marked "O.P." most likely originates from an optic phonon.

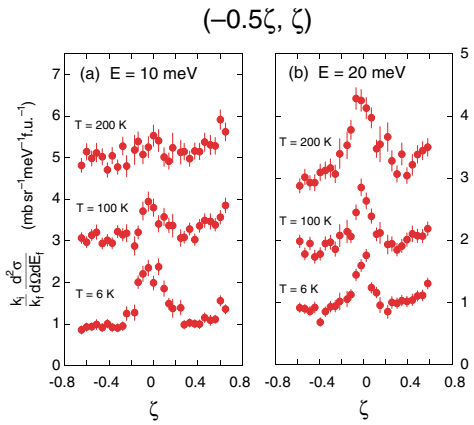

FIG. 3 (color online). Temperature dependence of the intensity at $\mathbf{Q}_{2D} = (0, 0)$ sampled at average energies of (a) 10 meV, and (b) 20 meV. The constant-energy cuts are taken along the line marked X in Fig. 1. The 100 and 200 K data have been displaced vertically for clarity. The displacements relative to the 6 K data are, respectively, (a) 2 and 3.5 units and (b) 1 and 2 units.

Figs. 3(a) and 3(b). The data presented in these plots are cuts through (0, 0) along the line marked X in Fig. 1. The temperature dependence is shown at average energies of 10 and 20 meV, respectively. The peak in the 10 meV cut is seen to decrease with temperature, and at 200 K is almost indistinguishable from the background. By contrast, the 20 meV peak increases with temperature.

The increase in intensity with temperature of the 20 meV peak suggests that this scattering arises from a bosonic excitation, such as a phonon. The scattering intensity is then expected to vary in proportion to the factor $\{1 - \exp(-\hbar\omega/k_B T)\}^{-1}$ [21], which increases by ~50% from 6 to 200 K. This increase is consistent with the data in Fig. 3(b). As there is currently no evidence for magnetic order at temperatures as high as 200 K in $Na_{0.75}CoO_2$ [19], the most likely origin of the 20 meV peak is an optic phonon.

On the other hand, the temperature dependence of the low energy feature suggests a magnetic origin because magnetic correlations decrease with temperature. The fact that the scattering is localized about $\mathbf{Q}_{2D} = (0, 0)$ implies that the correlations are ferromagnetic within the *ab* plane.

Having concluded that the low energy signal at $\mathbf{Q}_{2D} = (0, 0)$ corresponds to 2D ferromagnetic correlations, we now turn to its energy spectrum. Figure 4 displays a set of constant-energy cuts along the line marked X in Fig. 1 through the data collected at $T = 6$ K. The 6.5 meV cut shows a single peak centered at (0, 0), but with increasing energy the peak broadens and decreases in amplitude. In addition, the line shapes in the 10 and 14 meV cuts are distinctly flattopped, suggestive of two almost-resolved peaks on either side of $\zeta = 0$. Although the extent of our data is limited, it is clear that the magnetic scattering is highly dispersive and that it extends above 16 meV into the energy range where the optic phonon dominates the signal.

Finally, we consider the energy-integrated cross section, and compare it with the local-moment sum rule.

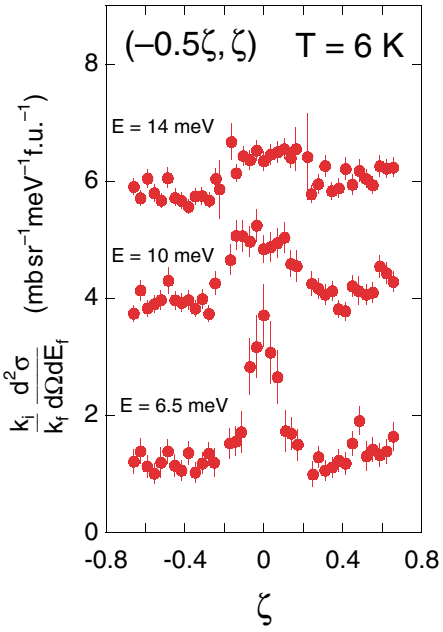

FIG. 4 (color online). Constant-energy cuts taken along the line marked X in Fig. 1. The 10 and 14 meV data have been displaced vertically by 3 and 5 units, respectively, for clarity.

Integrating the magnetic signal between 5 and 16 meV and averaging the result over one 2D Brillouin zone, we obtain ~ 1 mb sr^{-1} f.u.$^{-1}$. Neglecting the magnetic form factor, the energy-integrated, $\mathbf{Q}$-averaged scattering from a system of local moments with spin S is $\Sigma = \frac{1}{6}(\gamma r_0)^2 g^2 S(S+1)$ per spin, where $\gamma = 1.913$, $r_0 = 2.818 \times 10^{-15}$ m, and g is the Landé factor [21]. Taking as a reference the values $S = \frac{1}{2}$ and $g = 2$, we find $\Sigma = 145$ mb sr^{-1} spin^{-1}. In $Na_{0.75}CoO_2$ only a quarter of the Co ions carry a spin, on average, so this would reduce the expected cross section to ~ 36 mb sr^{-1} f.u.$^{-1}$. This is much larger than the inelastic scattering cross section we have observed, which suggests that there is considerable spectral weight outside the energy range probed in our experiment. Some of this will undoubtedly be at higher energies, since the measured spectrum appears to extend above 16 meV, but we would also expect some of the weight to be below 2 meV in the form of elastic or quasielastic scattering. In particular, although we collected elastic scattering data over a wide range of reciprocal space, we did not probe along the $(0, 0, l)$ line, so any Bragg peaks associated with in-plane ferromagnetic order could not have been measured. Full 3D ferromagnetic order is excluded by the magnetization data [19], but a spin arrangement with in-plane ferromagnetic order and a spin-density wave modulation perpendicular to the planes, e.g., an antiferromagnetic stacking along the c axis, would be compatible with our results.

The measurements reported here show conclusively that there exist strong ferromagnetic in-plane correlations in $Na_{0.75}CoO_2$, with an energy scale much larger than that set by the observed magnetic ordering temperature ($T_m = 22$ K [19]). Interestingly, the excitation spectrum resembles that found in nearly ferromagnetic metals, such as Ni_3Ga [23] and Pd [24], characterized by strongly damped or overdamped ferromagnons [25]. This finding is in remarkable accord with the picture described by Singh based on density-functional calculations in the local-density approximation (LDA) [17,18]. He predicts a weak itinerant ferromagnetic ground state for all doping levels in the range $x = 0.3$–0.7, and suggests that quantum spin fluctuations would in practice suppress the tendency for ordering. The spin excitation spectrum would then resemble that of overdamped ferromagnons, consistent with what is observed here.

There is good reason to believe that the ferromagnetic correlations found in Na_xCoO_2 will also be present in the superconducting compound, and may therefore play a role in the mechanism of superconductivity. The LDA calculations, which successfully described the present results, also predict a ferromagnetic ground state with the strained cell and Na doping of the hydrated superconductor [18]. This, together with the evidence reported for unconventional superconductivity [5], raises the possibility of p-wave spin-triplet pairing, a state thought to occur in Sr_2RuO_4 [26]. Unlike the ruthenate, however, the superconductivity in hydrated Na_xCoO_2 has not been reported sensitive to impurities, and the most prominent spin fluctuations in Sr_2RuO_4 are not ferromagnetic but instead have an incommensurate wave vector [27]. Nevertheless, the proximity to a ferromagnetic phase in each case suggests the mechanism of superconductivity in the two materials may share some common features.

We thank Martin Long, Chris Hooley, and Andy Mackenzie for insightful discussions. This work was supported by the Engineering & Physical Sciences Research Council of Great Britain.

*Electronic address: a.boothroyd1@physics.ox.ac.uk
URL: http://xray.physics.ox.ac.uk/Boothroyd

[1] I. Terasaki, Y. Sasago, and K. Uchinokura, Phys. Rev. B **56**, R12685 (1997).
[2] K. Takada *et al.*, Nature (London) **422**, 53 (2003).
[3] Y. Wang *et al.*, Nature (London) **423**, 425 (2003).
[4] R. E. Schaak *et al.*, Nature (London) **424**, 527 (2003).
[5] T. Waki *et al.*, cond-mat/0306036; T. Fujimoto *et al.*, Phys. Rev. Lett. **92**, 047004 (2004); K. Ishida *et al.*, J. Phys. Soc. Jpn. **72**, 3041 (2003); W. Higemoto *et al.*, cond-mat/0310324; Y. Kobayashi, M. Yokoi, and M. Sato, cond-mat/0305649.
[6] G. Baskaran, Phys. Rev. Lett. **91**, 097003 (2003).
[7] B. Kumar and B. S. Shastry, Phys. Rev. B **68**, 104508 (2003).
[8] M. Ogata, J. Phys. Soc. Jpn. **72**, 1839 (2003).
[9] C. Honerkamp, Phys. Rev. B **68**, 104510 (2003).
[10] Q.-H. Wang *et al.*, Phys. Rev. B **69**, 092504 (2004).
[11] P. W. Anderson, Science **235**, 1196 (1987).
[12] H. Sakurai *et al.*, Phys. Rev. B **68**, 132507 (2003); T. Fujimoto *et al.*, Phys. Rev. Lett. **92**, 047004 (2004).
[13] R. Ray *et al.*, Phys. Rev. B **59**, 9454 (1999).
[14] A. Tanaka and X. Hu, Phys. Rev. Lett. **91**, 257006 (2003).
[15] H. Ikeda, Y. Nisikawa, and K. Yamada, J. Phys. Soc. Jpn. **73**, 17 (2004).
[16] Y. Tanaka, Y. Yanase, and M. Ogata, J. Phys. Soc. Jpn. **73**, 319 (2004).
[17] D. J. Singh, Phys. Rev. B **61**, 13397 (2000).
[18] D. J. Singh, Phys. Rev. B **68**, 020503(R) (2003).
[19] T. Motohashi *et al.*, Phys. Rev. B **67**, 064406 (2003).
[20] D. Prabhakaran *et al.*, cond-mat/0312493.
[21] G. L. Squires, *Introduction to the Theory of Thermal Neutron Scattering* (Cambridge University Press, Cambridge, England, 1978).
[22] The reciprocal lattice vectors are defined as $\mathbf{a}^* = [(2\pi)/a](2/\sqrt{3})\hat{\mathbf{x}}$ and $\mathbf{b}^* = [(2\pi/a)][(1/\sqrt{3})\hat{\mathbf{x}} + \hat{\mathbf{y}}]$, where $\hat{\mathbf{x}}$ and $\hat{\mathbf{y}}$ are orthonormal vectors and $a = 2.83$ Å is the lattice parameter of the triangular lattice.
[23] N. R. Bernhoeft *et al.*, Phys. Rev. Lett. **62**, 657 (1989).
[24] R. Doubble, Ph.D. thesis, University of Bristol, 1998.
[25] S. Doniach, Proc. Phys. Soc. **91**, 86 (1967).
[26] Y. Maeno *et al.*, Nature (London) **372**, 532 (1994); A. P. Mackenzie and Y. Maeno, Rev. Mod. Phys. **75**, 657 (2003).
[27] Y. Sidis *et al.*, Phys. Rev. Lett. **83**, 3320 (1999).